PROCEEDINGS OF SCIENCE

Collider Studies on Jet Physics and Heavy Flavor Properties

Vieri Candelise[*†]
University of Trieste, INFN Trieste
vieri.candelise@ts.infn.it

The Large Hadron Collider at CERN is the world's most efficient jet factory. In this report the properties of jets will be discussed, with focus on reconstructed jets in the ATLAS, CMS and LHCb experiments. After a brief introduction of jet physics at colliders, a selection of the results on inclusive QCD jet production cross sections, jets originated from the hadronization of b quarks and top quarks final states will be shown, with special attention on the comparisons with the Monte Carlo generators predictions at the highest possible order in perturbative QCD, using proton-proton collisions data at the center of mass energy $\sqrt{s} = 7$, 8 and 13 TeV. Details on the measurements of the running of the strong coupling constant as well as the differential cross sections for the inclusive jet production in ATLAS and CMS are presented. An overview of the state-of-art algorithms for the b-quark tagging, following the measurement of the b-jets production in association with a Z boson in CMS and the decay of a Z boson to bottom quarks in LHCb are shown. The top quark pair production physics is then introduced, and the cross section measurement in forward region with LHCb is shown. Finally, predictions of the color flow between quarks are tested using angular considerations in top events in ATLAS.

XXVI International Workshop on Deep-Inelastic Scattering and Related Subjects (DIS2018)
16-20 April 2018
Kobe, Japan

[*]Speaker.
[†]On behalf of the ATLAS, CMS and LHCb Collaborations.

PoS(DIS2018)237

1. Introduction: Phenomenology of Jets at Colliders

Jets are copiously produced at the LHC in high-energy proton collisions. They are an essential part of the physics program of the LHC experiments, and they give us unique information on the quarks and gluons produced in the hard scattering. The production of jets gives us an insight on perturbative and non-perturbative aspects of quantum chromodynamics (pQCD): at LHC, we can explore this perturbative regime with unprecedented energies. Of primary importance is the study of the parton density functions (PDFs) and the possibility to probe and extract the strong coupling constant α_S and to measure its running. Jets are the fundamental ingredient to test the higher order pQCD predictions in the Monte Carlo simulation programs, and they give us an important tool to compare next-to-leading and next-to-next-to leading order precision (NLO,NNLO) in the theoretical calculations. Finally, we can use final states with high jet multiplicities to tune Monte Carlo generators and to study the characteristics of the parton shower and hadronization of quarks. A vast phenomenology is associated to the physics of jets at colliders. The associated production of jets and vector bosons ($V = Z, W, H$) allows to test the Standard Model (SM) deeply, reaching the highest possible precision in the perturbative expansion of QCD. Moreover, several models beyond the SM have jets in the final state: new heavy resonances in the dijet system, dark matter production in association with a single jet, hadronic resonances and supersymmetry are just examples of an extended spectrum of possible theories that include jets in the final state. Of recent interest is the possibility of explore the boosted regime, where sub-structure algoritms allow to discriminate the presence of multiple jets within a single "wide" jet. This techniques are extremely useful for a boosted Higgs boson tagging in the $b\bar{b}$ final state, as well as searches with boosted heavy flavors and Higgs bosons.

2. Jet Reconstruction

Jets can be defined as a collimated sprays of stable particles arising from the fragmentation and hadronisation of quarks or gluons after a collision, evolving in time and space within a cone in the η-ϕ space. In ATLAS [1], CMS [2] and LHCb [3], jet reconstruction algorithms are used to combine the calorimetry and tracking information to define a jet object. For all the experiments, the anti-k_T clustering algorithm [4] is used. This algorithm is based on the relative distance between two particles in the jet, d_{ij}, and an iteration parameter R. The momentum space distance between the beam axis and the detected particle (d_{iB}) is also calculated, and the sequential clustering algorithms work by first finding the minimum of the entire set of distances between the i-th and j-th particles within the cone. If d_{iB} is the minimum, i is labelled a final jet and removed from the list of particles. This process is repeated until all particles are part of a jet. The advantage of this algorithm is that it is infrared and collinear safe. In CMS, the Particle Flow algorithm [5] uses all the information of sub-detectors to build the reconstructed object. In LHCb, the particle flow algorithm in the forward direction adds the precise tracking information using identified unstable mesons like Λ, K_S, π. In ATLAS, topological calorimeter-cell clusters are identified in order to create calorimeter jets, relying on the performances of the electromagnetic and hadronic calorimeters. The energy of the reconstructed jet must be corrected for several effects, including changing the energy and the momentum of the "true" originating particle. In ATLAS and CMS, the jet energy

is corrected also for pile-up interactions, the jet flavor composition and the absolute and relative jet energy scale. The correction are performed with data-driven methods, using $in-situ$ methods and relying on very well measured physics processes, such as the W and Z boson production. The precision reached as a function of the jet momentum is less than 2% for a momentum of 100 GeV in ATLAS [6] and CMS [7], and about 10 to 15 % in LHCb for momenta in the range 10-100 GeV.

3. Results on Inclusive Jet Production

3.1 Inclusive Jet Differential Cross Section at 13 TeV with ATLAS and CMS

Inclusive jet and dijet cross sections are measured in proton-proton collisions at a centre-of-mass energy of 13 TeV in ATLAS [8] and CMS [9], with an integrated luminosity of 3.2 fb^{-1} and 71 pb^{-1} respectively. The ATLAS measurement relies on reconstructed anti-k_T jets within a cone parameter of 0.4. The inclusive jet cross sections are measured as a function of the jet transverse momentum, covering the range from 100 GeV to 3.5 TeV, and the absolute jet rapidity up to |y|=3. Data are unfolded for detector effects using the Bayesian iterative algorithm, and the measured cross sections, corrected for the perturbative and non-perturbative electroweak effects, are compared to the theoretical calculations by NLOJet++ using the CT14, MMHT and NNPDF3.0 parton density function sets. An overall good agreement is seen in the NNLO comparisons, as shown in Fig. 1. In CMS, the double-differential inclusive jet cross section is measured as a function of jet transverse momentum p_T and seven bins of absolute jet rapidity |y|, using anti-k_T jets with two jet sizes, R, of 0.7 and 0.4, in a phase space region covering jet momentum up to 2 TeV and jet rapidity up to |y| = 4.7. Unfolded cross sections are compared to the perturbative QCD predictions by NNLOJet++ and Powheg [10] interfaced with Pythia8 [11] for the hadronization, using the CT14 PDF set. A good agreement is seen when the NLO predictions are tested over the full spectrum of the jet momentum (Fig.1).

3.2 Determination of the Strong Coupling with ATLAS and CMS

The strong coupling constant, α_S, is extracted from multi-jet final states in ATLAS and CMS using different techniques, using LHC data at 8 TeV. In ATLAS, the measurement is performed exploiting the sensitivity of the energy-energy correlation variables [12] and their associated asymmetries in multi-jet events, with an integrated luminosity of 20.2 fb^{-1}. The results are presented in bins of the scalar sum of the transverse momenta of the two leading jets, unfolded to particle level and compared to the pQCD predictions of Sherpa [13], Herwig++ [14] and Pythia8. The comparison shows excellent agreement within the uncertainties, and the value of α_S is extracted for different energy regimes, thus testing the running predicted in QCD up to scales over 1 TeV. A global fit to the transverse energy-energy correlation distributions yields $\alpha_S = 0.1162 \pm 0.0011(exp.)^{+0.0084}_{-0.0070}(theo.)$, while a global fit to the asymmetry distributions yields a value of $\alpha_S = 0.11960.0013(exp.)^{+0.0075}_{-0.0045}(theo.)$. In CMS, the extraction of α_S is performed by measuring the double-differential inclusive jet cross section [15] as a function of the jet transverse momentum and the absolute jet rapidity, using 8 TeV data corresponding to an integrated luminosity of 19.7 fb^{-1}. Anti-k_T jets with a size parameter of 0.7 in a phase space region covering jet momentum from 74 GeV up to 2.5 TeV and jet absolute rapidity up to 3.0. The low-momentum

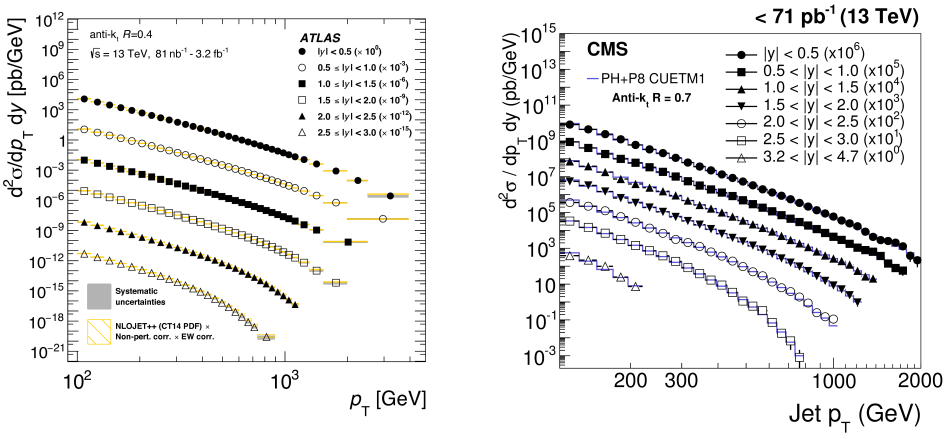

Figure 1: Left: ATLAS Inclusive jet cross sections as a function of p_T and y, for anti-k_T jets with R=0.4 [8]. The statistical uncertainties are smaller than the size of the symbols used to plot the cross-section values. The shaded areas indicate the experimental systematic uncertainties. The data are compared to NLO pQCD predictions calculated using NLOJET++ with $p_T$max as the QCD scale and the CT14 NLO PDF set, to which non-perturbative and electroweak corrections are applied. The hatched open boxes indicate the predictions with their uncertainties. Right: CMS double-differential inclusive jet cross section as function of jet p_T [9]. On the left, data (points) and predictions from NLOJet++ based on the CT14 PDF set corrected for the NP and electroweak effects (line) are shown. On the right, data (points) and predictions from POWHEG interfaced to PYTHIA8 with tune CUETPM1 (line) are shown. Jets are clustered with the anti-k_T algorithm (R= 0.7).

range between 21 and 74 GeV is also studied up to |y|= 4.7, using a dedicated data sample corresponding to an integrated luminosity of 5.6 pb^{-1}. The measured jet cross section is corrected for detector effects and compared to the predictions from perturbative QCD at next-to-leading order (NLO) using several PDFs sets, taking into account for the non-perturbative and electroweak corrections. The extracted value of the strong coupling constant evaluated at the Z boson mass is $\alpha_S(M_Z) = 0.1164 + 0.0060 - 0.0043$, where the errors include the PDF, scale, non-perturbative effects and experimental uncertainties, using the CT10 NLO PDFs. The results on the running of α_S obtained by ATLAS and CMS are shown in Fig.2.

4. Results with Jets originated from b Quarks

4.1 Heavy Flavor Tagging at Colliders

Identifying the flavor of a given jet is of extreme importance to access the b and c quark content of the event, explore final states with b-jets and expand our knowledge of perturbative QCD with heavy flavors. Several advanced techniques are used to discriminate b-jets. In ATLAS, the b-tagging is performed using track-based (impact parameter tag), soft-muon (discriminating muons from semi-leptonic b decays), and vertex based algorithms. High level taggers have been recently developed, exploiting the statistical power of multivariate analyses, combining the kinematic information based on tracks, particles and vertices of the event thus maximizing the b-tagging performance. A b-tagging efficiency of about 77% is achieved, with a mistag rate of light-flavored jets of less than 2% up to jets with momentum of 1 TeV. In LHCb, the b-tagging is performed by

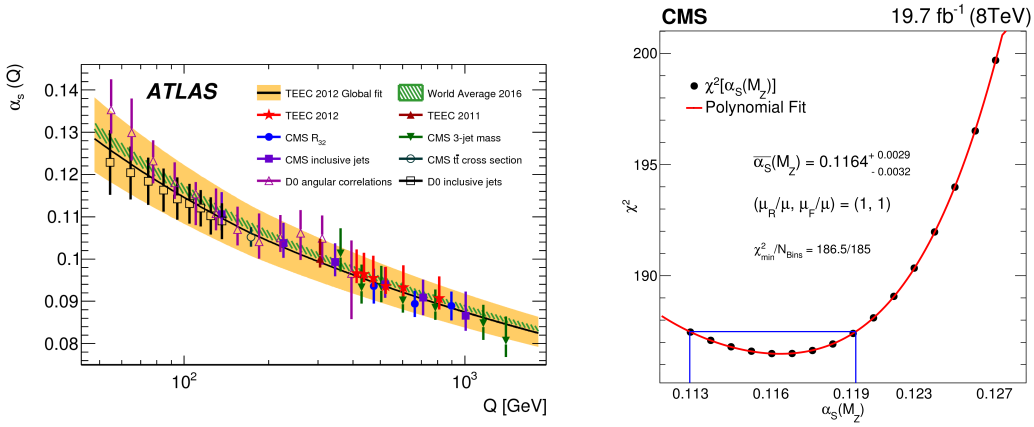

Figure 2: Left: ATLAS extraction of α_S obtained from fits to the energy correlation functions (red star points) with the uncertainty band from the global fit (orange full band) and the 2016 world average (green hatched band) [12]. Determinations from other experiments are also shown as data points. The error bars, as well as the orange full band, include all experimental and theoretical sources of uncertainty. Right: CMS extraction of α_S .The χ^2 minimization with respect to α_S by using the CT10 NLO PDF set and data from all rapidity bins [15]. The uncertainty is obtained from the $\alpha_S(M_Z)$ values for which χ^2 is increased by one with respect to the minimum value, indicated by the box. The curve corresponds to a fourth-degree polynomial fit through the available χ^2 points.

reconstructing the two-bodies vertices of the event, and merging the secondary vertex multi-body by linking tracks and their associated vertices. Secondary vertices and jets are selected within a distance in the $\eta - \phi$ plane of 0.5. The algorithm allows to reach a b-tagging efficiency of 65% and a mistag rate of less than 1%. In CMS, several taggers are available. The two principal ones are the Jet Probability, using the likelihood that a given jet is coming from the primary vertex using tracks, and the Combined Secondary Vertex (CVS), that combines, by means of a multi-variate analysis, the information of displaced tracks with the information on the secondary vertex associated to a jet. High level taggers, such as the "CSVv2" and the "deepCSV" are modifications of the standard CSV and they use neural and deep neural networks to perform the statistical combination of the parameters. With these high level taggers, an improvement of 4% in the b-tagging efficiency with respect to the standard taggers is achieved, with a mistag rate of 0.1%.

4.2 Observation of $Z \to b\bar{b}$ in LHC*b*

The Z boson decay to bottom quarks is one of the important *standard candles* of the Standard Model. Many physics processes within and beyond the Standard Model have an important QCD background of $Z \to b\bar{b}$. A clear example is the Higgs boson decay $H \to b\bar{b}$. While the ATLAS and CMS experiments have measured the $Z \to b\bar{b}$ cross section in their acceptance, a measurement of this important process in the forward region has been made recently by LHCb[16], thanks to its unique projective geometry. The measurement is made using 8 TeV data with an integrated luminosity of 2 fb^{-1}. Particle level b-tagged jets are selected in the pseudorapidity range of $2.2<\eta<4.2$, for jets with momentum greater than 20 GeV. The dijet invariant mass selected in this the range is $45<m_{jj}<165$ GeV. The huge background of QCD jets is taken into account by separating the

QCD jets from signal b-tagged jets through a Multivariate Analysis using a control region that is defined through observables related to the b-dijet system and to the associated balancing jet. The biggest contribution of systematic uncertainties arises from the jet flavor tagging efficiency (17%), jet energy corrections and trigger efficiency (2%). A simultaneous fit to the dijet invariant mass in the signal and control regions is performed to extract the cross section, as shown in Fig. 3. The extracted value of the $Z \to b\bar{b}$ cross section is $332 \pm 46 \pm 59$ pb is compared to the NLO prediction using aMCNLO interfaced with Pythia and using the NNPDF3.0 parton density function set. The comparison shows a very good agreement within the Standard Model prediction at NLO. The invariant mass distribution of the Z peak in the $b\bar{b}$ system is shown in Fig.3.

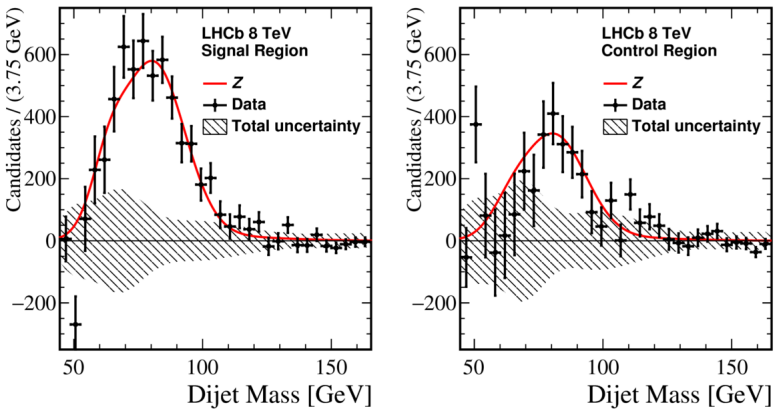

Figure 3: Background-subtracted distribution of the $Z \to b\bar{b}$ mass model in the (left) signal and (right) control regions. The one standard deviation total uncertainty band in the background-only hypothesis is also shown. including statistical and systematic uncertainties [16].

4.3 Associated Production of a Z boson and b-jets in CMS

The associated production of a Z boson and b quarks is an important test of perturbative QCD. The presence of a b quark in the perturbative expansion makes the pQCD challenging, since the b quark has a sizable effect in the final cross sections. Two models can be tested, using effective field theories with 4 flavors ($m_b \neq 0$) and 5 flavors ($m_b = 0$) in the initial state, namely 4FS and 5FS respectively. Moreover, the $Z + b$ process is an important background for many processes in the Standard Model and in new physics searches, such as the associated production of the Higgs boson in association with a vector boson (VH channel), searches for new heavy resonances decaying to ZH, Zbb, search for fourth generation of quarks (b'). The analysis is focused on the measurement of differential cross sections for Z plus at least one b-jet and Z plus at least two b-jets (separately) as a function of several kinematic observable characterizing the event, using 8 TeV CMS data with an integrated luminosity of 19.8 fb $^{-1}$[17]. Jets are tagged as b-jets using the CSV algorithm, and they are required to have $p_T > 30$ GeV and $\eta < 2.4$. The Z boson is selected through the invariant mass of the electron and muon pairs invariant mass and two categories are chosen: Z+($\geq 1b$) (Z1b) and Z+($\geq 2b$) (Z2b). Data are unfolded to particle level using the Singular Value Decomposition unfolding algorithm (SVD) and the dominant top quark background is estimated using data driven techniques. Unfolded cross sections are compared to the NLO predictions of MadGraph_aMCNLO

[18] interfaced with Pythia8, Madgraph+Pythia6 in the 4FS and 5FS, and to Powheg. Regions of the tested phase space are found to be in in general good agreement with the 5FS for the Z1b, while some tensions are present using the 4FS approach. For the Z2b sample, more statistics is needed to draw significant conclusions, but measured data agree with the 4 and 5 FS over the majority of the distributions under study. As an example, the differential cross section as a function of the ΔR between the leading and sub-leading b-jet (sensitive to pQCD) and the invariant mass of the $b\bar{b}$ system (sensitive to potential underlying new particles) are shown for the Z2b sample in Fig.4.

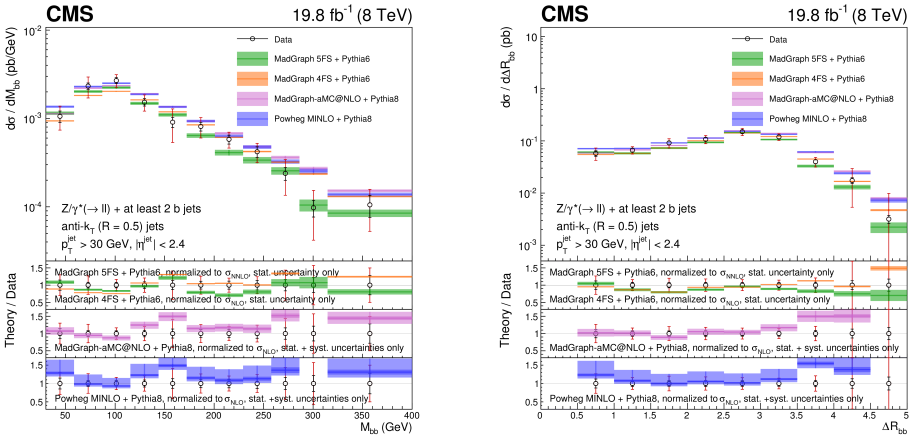

Figure 4: Left: Differential fiducial cross section for Z(2b) production as a function of $\Delta R(b\bar{b})$, compared with the MadGraph 5FS, MadGraph 4FS, MadGraph5_aMC@NLO, and Powheg theoretical predictions (shaded bands). For each data point the statistical and the total (sum in quadrature of statistical and systematic) uncertainties are represented by the double error bar. The width of the shaded bands represents the uncertainty in the theoretical predictions, and, for NLO calculations, the inner darker area represents the statistical component only. Right: Differential fiducial cross section for Z(2b) production as a function of the invariant mass of the b jet pair, $M(b\bar{b})$ compared with the MadGraph 5FS, MadGraph 4FS, MadGraph5_aMC@NLO, and Powheg theoretical predictions (shaded bands). For each data point the statistical and the total (sum in quadrature of statistical and systematic) uncertainties are represented by the double error bar. The width of the shaded bands represents the uncertainty in the theoretical predictions, and, for NLO calculations, the inner darker area represents the statistical component only [17].

5. Jet Physics with Top Quarks

5.1 Top Quark Physics at Colliders

The top quark plays a special role in the physics program of LHC. Given its mass, the coupling of the top quark to the Higgs boson is the highest one in the Standard Model, and this fact makes the top physics particularly interestings for the understanding of the of the electroweak symmetery breaking, the Higgs boson properties and the understanding of the hierarchy problem. Nevertheless, the top quark measurements play an important role in pQCD, where the differential cross sections allow to a deep understanding of the perturbative corrections at NNLO and NNLL precision, the parton shower modelization and tuning of Monte Carlo generators. Moreover, the top quark is a principal actor in the search of physics beyond the Standard Model in a huge variety of theoretical models. The LHC and its experiments are a perfect environment for top production. The main

production in proton-proton collisions occurs through the gluon-gluon fusion process (90%), and a very high rate of top quarks is available at LHC (about 30 millions produced only in 2016). The $t\bar{t}$ cross section at 13 TeV is measured with a combined (ATLAS+CMS) precision of about 5.5 %, overcoming the NNLO+NNLL precision for the first time. LHCb measured the top quark in the forward region for the first time at 13 TeV, reaching a precision of 20% in the cross section measurement.

5.2 Measurement of the Forward Top Quark Pairs Cross Section in LHCb

The unique forward acceptance of the LHCb detector allows measurements of the top quark in a phase space inaccessible to ATLAS and CMS. The production of top quarks in this region receives a higher contribution from quark-antiquark annihilation than in the central region, thus accessing higher values of Bjorken-x,experimentally poorly known because of the large PDF errors. For this reason, precise measurements of top quark production at LHCb can be used constrain PDFs in this region. Moreover, the greater contribution from quark-initiated produces also a larger expected top quark charge asymmetry in the forward region. The forward top production cross section is measured in LHCb using proton collision data at 13 TeV for an integrated luminosity of 1.93 fb^{-1} through the $e\mu b$ final state [19]. The cross section is measured in a fiducial region where both leptons have a p_T >20 GeV and 2<η<4.5. The relative distance in the $\eta-\phi$ plane between the two leptons is required to be ΔR <0.1. The b-tagged jets, identified using secondary vertex algorithms, is required to be separated from both leptons by ΔR<0.5, and to have a transverse momentum greater than 20 GeV and a pseudorapidity between 2.2 and 4.2. The measured cross section, extrapolated to top quark level, is $\sigma(t\bar{t}) = 126 \pm 19(stat.) \pm 16(syst.) \pm 5(lumi)$ fb, where the uncertainties in the brackets are, in order, statistical, systematic and due to luminosity determination. The measurement is found to be compatible with the Standard Model prediction within 2 standard deviations. The $e\mu b$ invariant mass distribution is shown in Fig.5, together with the measured cross section in femtobarn compared to the theoretical calculations of Powheg, aMC@NLO [22] and MCFM. The yellow and green bands represent the $\pm 1\sigma$ standard deviation intervals.

5.3 Color Flow Using Jet-Pull Observables in $t\bar{t}$ Events

The direct measurement of the interactions that occur between quarks and gluons is very difficult to obtain, since only color neutral hadrons can be measured. The color connections (Color-Flows) between particles can affect the structure of the emitted radiation and therefore also the structure of the resulting jets. A smaller effect arises in the process of hadronisation, that usually relies on QCD models in the Monte Carlo generators. A direct measurement of the Color Flows between particles is an important test of the QCD. Moreover, the extracted color connection information may be used as a powerful tool to discriminate between different event topologies with different color structure, and thus quantifying irreducible jet-based backgrounds by correctly assigning a given jet to the desired physics process, for example distinguishing b-jets from different decays in the $t\bar{t}H$ process with $H \to b\bar{b}$. In ATLAS the color-flow measurements is made using the so called Jet-Pull angle (θ_P) and Jet-Pull magnitude ($\vec{P}$) , all derived from the Jet-Pull angular moment [20], defined as the vector that connects the j constituent of a given jet with the axis of the second jet in the $\Delta\phi(jj) - \Delta y(jj)$ plane. The extraction of θ_P allows to relate the color structure of a jet to the global structure of the dijet syste. The ATLAS measurement [21] is performed in top

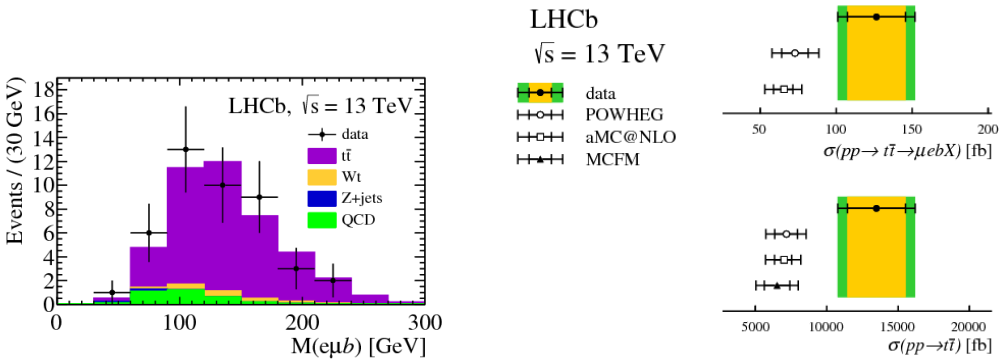

Figure 5: Left: The combined invariant mass of the muon, electron and b-jet in data compared to the expected contributions. The $t\bar{t}$ signal yield is determined to be the number of selected events minus the sum of the expected backgrounds. Right: Graphical comparison of the measured cross sections with the predictions from the aMC@NLO, powheg and mcfm generators. For the data, the inner error band represents the statistical uncertainty, and the outer the total, while for the theoretical predictions, the inner band represents the scale uncertainty and the outer represents the total. The prediction is shown (above) for the muon, electron and jet fiducial, and (below) for the top fiducial region [19].

quark pair events with one leptonically decaying W boson and one hadronically decaying W boson, with proton-proton data with an integrated luminosity of 36.1fb^{-1} at $\sqrt{s}$ = 13TeV. Two system are considered: in the first one, two color connected jets, corresponding to values of ($\theta_P(jj)$) close to zero, are taken from the color singlet $W \to jj$ in $t\bar{t}$ events. In the second case, uncorrelated colors jet pairs are taken through $b\bar{b}$ events in $t\bar{t}$ events, where non-zero values of $\theta_P(jj)$ are expected. The two cases are reported in Fig.6, where the normalised fiducial cross sections as a function of θ_P are compared to the theoretical predictions of several event generators at the NLO precision. While a disagreement with respect to the Standard Model is seen in both distributions, different models of hadronization considerably improve the description of the color-sensitive observables, and further studies are foreseen for this important measurement.

6. Conclusions

Jet physics at colliders is an essential part of the scientific program of modern particle physics experiments. At the LHC, several tests of the perturbative QCD have been made using jets in ATLAS, CMS and LHCb. State-of-art jet reconstruction in the three experiments is used, and thanks to performing algorithms it is possible to reach outstanding precision in the jet energy measurements and corrections. Jet measurements at colliders give us information on the precision of the Standard Model measurements as well as insight on potential beyond the Standard Model processes and potential new particle discoveries. Inclusive jet cross sections open up to a deep test of the most recent calculations with Monte Carlo generator measurements of the strong coupling constant at new energies. Heavy flavor tagging exploits advanced statistical techniques to combine all the relevant kinematic information of the event to distinguish b/c-quarks from light flavors and gluons. Thanks to these tools, several Standard Model tests are possible, and unprecedented precision at hadron colliders is reached in the bosons hadronic decay, boson plus jets and heavy flavors and color-flow

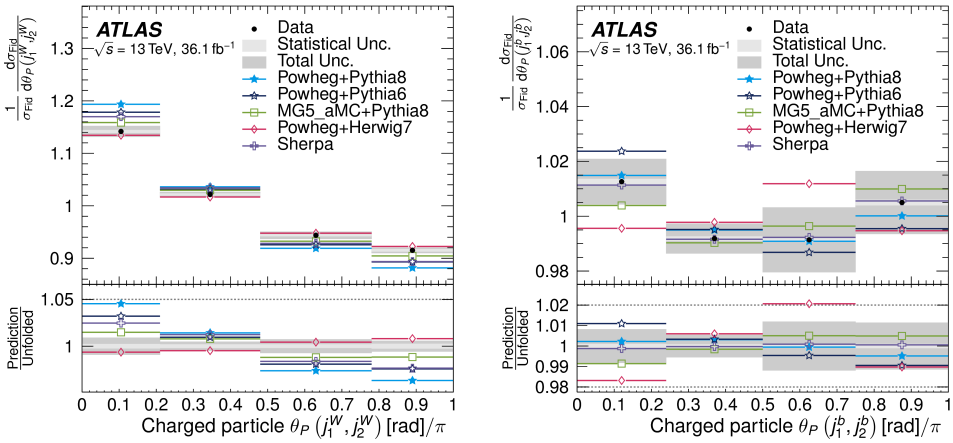

Figure 6: Left: Normalised fiducial differential cross sections as a function of the pull angle for the hadronically decaying W boson daughters. The data are compared to several Standard Model predictions. Right: Normalised fiducial differential cross sections as a function of the pull angle for the $b\bar{b}$ system. All the distributions refer to $t\bar{t}$ events [20].

measurements. Of particular importance is the possibility to reach the NLO and NNLO precision also in the forward region thanks to the LHCb geometry. The presented measurements are only a demonstrative example of the impressive set of high level scientific results available on jet physics in ATLAS, CMS and LHCb.

References

[1] G. Aad *et al.* [ATLAS Collaboration], "The ATLAS Experiment at the CERN Large Hadron Collider", JINST 3 (2008) S08003. doi:10.1088/1748-0221/3/08/S08003

[2] S. Chatrchyan et al. [CMS Collaboration], "The CMS Experiment at the CERN LHC", JINST 3 (2008) S08004. doi:10.1088/1748-0221/3/08/S08004

[3] A. A. Alves, Jr. et al. [LHCb Collaboration], "The LHCb Detector at the LHC", JINST 3 (2008) S08005. doi:10.1088/1748-0221/3/08/S08005

[4] M. Cacciari, G. P. Salam and G. Soyez, "The Anti-k(t) jet clustering algorithm", JHEP **0804** (2008) 063 doi:10.1088/1126-6708/2008/04/063 [arXiv:0802.1189 [hep-ph]].

[5] CMS Collaboration "Commissioning of the Particle-flow Event Reconstruction with the first LHC collisions recorded in the CMS detector" CMS-PAS-PFT-10-001 https://cds.cern.ch/record/1247373

[6] M. Aaboud *et al.* [ATLAS Collaboration], "Jet energy scale measurements and their systematic uncertainties in proton-proton collisions at $\sqrt{s} = 13$ TeV with the ATLAS detector", Phys. Rev. D **96** (2017) no.7, 072002 doi:10.1103/PhysRevD.96.072002 [arXiv:1703.09665 [hep-ex]].

[7] V. Khachatryan *et al.* [CMS Collaboration], "Jet energy scale and resolution in the CMS experiment in pp collisions at 8 TeV", JINST **12** (2017) no.02, P02014 doi:10.1088/1748-0221/12/02/P02014 [arXiv:1607.03663 [hep-ex]].

[8] M. Aaboud *et al.* [ATLAS Collaboration], "Measurement of inclusive jet and dijet cross-sections in proton-proton collisions at $\sqrt{s} = 13$ TeV with the ATLAS detector", JHEP **1805** (2018) 195 doi:10.1007/JHEP05(2018)195 [arXiv:1711.02692 [hep-ex]].

[9] V. Khachatryan *et al.* [CMS Collaboration], "Measurement of the double-differential inclusive jet cross section in proton-proton collisions at $\sqrt{s}$ = 13TeV", Eur. Phys. J. C **76** (2016) no.8, 451 doi:10.1140/epjc/s10052-016-4286-3 [arXiv:1605.04436 [hep-ex]].

[10] S. Alioli, P. Nason, C. Oleari and E. Re, "A general framework for implementing NLO calculations in shower Monte Carlo programs: the POWHEG BOX", JHEP 1006 (2010) 043 doi:10.1007/JHEP06(2010)043 [arXiv:100 2.2581 [hep-ph]].

[11] T. Sjostrand, S. Mrenna and P. Z. Skands, "A Brief Introduction to PYTHIA 8.1", Comput.Phys.Commun. 178 (2008) 852 doi:10.1016/j.cpc.2008.01.036 [arXiv:0710.3820 [hep-ph]].

[12] M. Aaboud *et al.* [ATLAS Collaboration], "Determination of the strong coupling constant α_s from transverse energy-energy correlations in multijet events at $\sqrt{s} = 8$ TeV using the ATLAS detector", Eur. Phys. J. C **77** (2017) no.12, 872 doi:10.1140/epjc/s10052-017-5442-0 [arXiv:1707.02562 [hep-ex]].

[13] T. Gleisberg, S. Hoeche, F. Krauss, M. Schonherr, S. Schumann, F. Siegert and J. Winter, "Event generation with SHERPA 1.1", JHEP 0902 (2009) 007 doi:10.1088/1126-6708/2009/02/007 [arXiv:0811.4622 [hep-ph]].

[14] M. Bahr et al., "Herwig++ Physics and Manual", Eur. Phys.J.C 58 (2008) 639 doi:10.1140/epjc/s10052-008-0798-9 [arXiv:0803.0883 [hep-ph]].

[15] V. Khachatryan *et al.* [CMS Collaboration], "Measurement and QCD analysis of double-differential inclusive jet cross sections in pp collisions at $\sqrt{s} = 8$ TeV and cross section ratios to 2.76 and 7 TeV", JHEP **1703** (2017) 156 doi:10.1007/JHEP03(2017)156 [arXiv:1609.05331 [hep-ex]].

[16] R. Aaij *et al.* [LHCb Collaboration], "First observation of forward $Z \to b\bar{b}$ production in pp collisions at $\sqrt{s} = 8$ TeV", Phys.Lett.B 776 (2018) 430 doi:10.1016/j.physletb.2017.11.066 [arXiv:1709.03458 [hep-ex]].

[17] V. Khachatryan et al. [CMS Collaboration], "Measurements of the associated production of a Z boson and b jets in pp collisions at $\sqrt{s} = 8$ TeV" Eur. Phys. J. C 77 (2017) no.11, 751 doi:10.1140/epjc/s10052-017-5140-y [arXiv:1611.06507 [hep-ex]].

[18] J. Alwall et al., "The automated computation of tree-level and next-to-leading order differential cross sections, and their matching to parton shower simulations", JHEP 1407 (2014) 079 doi:10.1007/JHEP07(2014)079 [arXiv:1405.0301 [hep-ph]].

[19] R. Aaij *et al.* [LHCb Collaboration], "Measurement of forward top pair production in the dilepton channel in pp collisions at $\sqrt{s} = 13$ TeV',' arXiv:1803.05188 [hep-ex].

[20] G. Aad et al. [ATLAS Collaboration], "Measurement of colour flow with the jet pull angle in $t\bar{t}$ events using the ATLAS detector at $\sqrt{s} = 8$ TeV',' Phys. Lett.B 750 (2015) 475 doi:10.1016/j.physletb.2015.09.051 [arXiv:1506.05629 [hep-ex]].

[21] M. Aaboud et al. [ATLAS Collaboration], "Measurement of colour flow using jet-pull observables in $t\bar{t}$ events with the ATLAS experiment at $\sqrt{s} = 13$ TeV',' arXiv:1805.02935 [hep-ex].

[22] R. Frederix and S. Frixione, "Merging meets matching in MC@NLO", JHEP 1212 (2012) 061 doi:10.1007/JHEP12(2012)061 [arXiv:1209.6215 [hep-ph]].